Exploring The Photoelectric Effect with Mercury Vapor and The Photoconductivity of Cadmium Sulfide

James Atkisson and Zhongzhe Li
Department of Physics and Astronomy, The University of North Carolina at Chapel Hill
(Physics 281, Group ζ)
(Dated: September 14, 2025)

This experiment aimed to explore two objectives: verifying the key principles of the photoelectric effect and investigating the photoconductivity of a Cadmium Sulfide (CdS) sample. For the photoelectric effect, we confirmed several of Einstein's predictions, including the dependence of stopping potential on light frequency rather than intensity, the existence of some threshold frequency, and the relationship between the maximum kinetic energy and incident photon energy. Our experimental data showed that as the wavelength increased, the stopping potential decreased and eventually dropped to zero, showing there was some cutoff wavelength. Light intensity was found to affect the number of emitted electrons, but not their individual energies, confirming that photon energy is independent of light intensity. Using filtered data to minimize the ambient noise, we measured Planck's constant to be $(6.503 \pm 0.51) \times 10^{-34}$ Joule seconds, within 1.86% of the accepted value, showing high experimental accuracy. In our exploration of photoconductivity, voltage current measurements indicated Ohmic behavior in the CdS sample, and the photocurrent was observed to vary linearly with the cosine squared of the polarization angle, verifying Malus' Law. Furthermore, Wall-Plug efficiency assessments showed that while higher bias voltages increased photocurrent, lower voltages yielded better efficiency, emphasizing the need for balancing input and output power for optimization. This experiment not only verified core concepts that would later be known as quantum theory, but it also demonstrated how these quantum scale interactions influence the electrical properties of semiconductor materials, forming the groundwork for technologies such as photovoltaics, optical sensors, and quantum computing systems. Our results overall reflect a fundamental refutation of classical physics, and how quantum physics connects with material science, driving foundational discoveries that continue to inspire technological innovation.

I. INTRODUCTION

Light has long fascinated scientists—not only for its ability to illuminate the world but also for the surprising ways it interacts with matter. In this experiment, we explore two fundamental phenomena that reveal the quantum and optoelectronic nature of light: the photoelectric effect and photoconductivity.

The photoelectric effect, first observed by Heinrich Hertz in 1887 and explained by Albert Einstein in 1905, challenged classical electromagnetic theory. Einstein proposed that light behaves not only as a wave but also as discrete energy packets called photons. When light of sufficiently high frequency strikes a metal surface, these photons can transfer their energy to electrons, ejecting them from the material. This phenomenon occurs only if the photon energy exceeds a material-specific threshold, independent of light intensity. This led to a new understanding of light and supported the emerging field of quantum mechanics.

In the first part of the experiment, we examine the photoelectric effect using a spectrometer and photodetector apparatus. By illuminating the detector with various spectral lines and measuring the resulting stopping potential, we confirm the quantum behavior of light and experimentally determine Planck's constant, a cornerstone of quantum theory.

In contrast, photoconductivity focuses on how light increases electrical conductivity in a semiconductor. In the second part of the experiment, we investigate cadmium sulfide (CdS), a material sensitive to visible light. When photons with sufficient energy are absorbed, they excite electrons from the valence band to the conduction band, creating free charge carriers—electrons and holes—that enhance conductivity. This process is central to technologies like solar cells and light sensors.

We analyze how the photocurrent in CdS depends on both the applied voltage and the intensity of incident light. By using polarizers and applying Malus's Law, we observe a cosine-squared relationship between light intensity and photocurrent, further validating the photoconductive model. We also evaluate the overall system efficiency by comparing the input power to the light source and the output power from the photoconductor.

Together, these experiments illustrate two sides of light-matter interaction—liberating electrons from a surface and generating mobile carriers within a material. This dual perspective deepens our understanding of light's role in both fundamental physics and modern optoelectronic applications.

Beyond advancing fundamental physics, the principles demonstrated in this experiment underpin a wide range of practical technologies. The photoelectric effect is the basis for devices such as photomultiplier tubes, solar panels, and light sensors, which convert light into usable electrical energy. Similarly, photoconductivity enables the function of photoresistors, optical switches, and imaging devices like charge-coupled devices (CCDs). Understand-

ing these mechanisms not only deepens scientific insight but also drives innovation in renewable energy, telecommunications, and sensor technologies.

II. THEORETICAL BACKGROUND

A. Photoelectric Effect

When light of frequency f strikes a material, the maximum kinetic energy $K_{\max}$ of the emitted photoelectrons is given by

$$K_{\max} = hf - \Phi, \tag{1}$$

where:

- h is Planck's constant (J s),
- f is the frequency of incident light (Hz),
- Φ is the material's work function (J).

The kinetic energy relates to the stopping potential V_0 by

$$K_{\max} = eV_0, \tag{2}$$

where e is the elementary charge (1.602×10^{-19} C). Thus,

$$eV_0 = hf - \Phi, \tag{3}$$

which rearranges to

$$V_0 = \frac{h}{e}f - \frac{\Phi}{e}. \tag{4}$$

To relate the frequency f to measurable experimental quantities, we use the diffraction grating equation. When light is diffracted by a grating with spacing d, the condition for constructive interference is

$$d\sin\theta = n\lambda, \tag{5}$$

where:

- d is the distance between adjacent slits (grating spacing) (m),
- θ is the diffraction angle (°),
- n is the diffraction order (integer),
- λ is the wavelength of light (m).

Solving for λ gives

$$\lambda = \frac{d\sin\theta}{n}, \tag{6}$$

thus the frequency is

$$f = \frac{c}{\lambda} = \frac{cn}{d\sin\theta}, \tag{7}$$

where c is the speed of light ($3.00\times10^8\,\mathrm{m\,s^{-1}}$).

B. Photoconductivity

Photoconductivity occurs in semiconductors when incident photons excite electrons across the material's band gap. The band gap E_g is the minimum energy required to promote an electron from the valence band to the conduction band. The basic condition for photoconductivity is

$$hf \geq E_g, \tag{8}$$

where all terms are as previously defined.

The steady-state excess carrier concentration Δn_e (number of additional mobile electrons per unit volume) is determined by

$$\Delta n_e = \frac{\eta_{qe}\Phi\tau}{AL}, \tag{9}$$

where:

- η_{qe} is the quantum efficiency (dimensionless, fraction of photons generating carriers),
- Φ is the incident photon flux (photons/m^2/s),
- τ is the carrier lifetime (average time before recombination) (s),
- A is the cross-sectional area of the sample (m^2),
- L is the length of the material along the current flow (m).

The change in conductivity $\Delta\sigma$ is given by

$$\Delta\sigma = q\mu_e\Delta n_e, \tag{10}$$

where:

- q is the elementary charge (1.602×10^{-19} C),
- μ_e is the electron mobility ($\mathrm{m^2\,V^{-1}\,s^{-1}}$).

The resulting photocurrent i_p under an applied voltage V is

$$i_p = \frac{q\mu_e\eta_{qe}\tau}{L^2}V\Phi, \tag{11}$$

where V is the applied bias voltage (V).

The light intensity after passing through a polarizer obeys Malus's Law:

$$I = I_0\cos^2\theta, \tag{12}$$

where:

- I is the transmitted intensity ($\mathrm{W\,m^{-2}}$),
- I_0 is the initial intensity,
- θ is the angle between the light polarization and the polarizer axis.

Thus, the photocurrent follows

$$i_p \propto \cos^2\theta. \tag{13}$$

Finally, the wall-plug efficiency η is given by

$$\eta = \frac{I_{\text{photo}} V_{\text{bias}}}{V_{\text{bulb}} I_{\text{bulb}}}, \tag{14}$$

where:

- I_{photo} is the photocurrent (A),
- V_{bias} is the bias voltage applied to the photoconductor (V),
- V_{bulb} is the voltage applied to the light source (V),
- I_{bulb} is the current through the light source (A).

III. METHODS

A. Photoelectric Effect

The photoelectric effect apparatus used in this experiment revolves around a goniometer spectrometer, which was used to measure the spectrum of mercury vapor. The materials used for this are described below.

- Photoelectric effect goniometer spectrometer apparatus, with the following components mounted on the large aluminum rotating stage
  - Mercury vapor lamp with lens and 610 lines/mm diffraction grating
  - Pasco Scientific model AP-9368 h/e photodetector apparatus paired with two 9V batteries
- Red, green, blue, and yellow optical filters
- Variable transmission optical filter
- Computer with USB-A port running Logger Pro (Ver. 3.16.2 was used)
- Vernier LabQuest mini and USB cable
- Vernier voltage probe
- Digital multimeter
- Two banana cables

1. Apparatus Setup

One of the most important parts of this particular exploration is the setup of the goniometer spectrometer apparatus. An image of the base setup can be seen in Fig. 1. Before the experiment is conducted, the batteries of the photodetector apparatus must be tested. The particular photodetector apparatus used in this experiment contains an amplifier. This is because when the emitted mercury vapor light hits the target material inside the photodetector, it ejects electrons because of the photoelectric effect. These ejected electrons create a small current, however this is too small for our equipment to directly detect. As such the amplifier increases the voltage signal generated by the current, so that it can be accurately measured by the voltage probe. The photodetector apparatus was powered on, and a digital multimeter was used to verify that the potential drop between the battery test banana plug and ground banana plug was above 6V. Once verified, LoggerPro was launched on a computer with a USB-A port, and the LabQuest mini was plugged in. The voltage probe was connected to the LabQuest, and was then wired to monitor the potential across the output ports of the photodetector. It is important to note that the photodetector must be zeroed before any measurements. This is because the photodetector is a capacitor that is charged by a current of photoelectrons ejected from the target material in the detector. By pressing the "push to zero" button, the plates of the capacitor are shorted, which allows it to discharge. Releasing this button allows the capacitor to charge.

The yellow light that exits the mercury vapor lamp travels through a narrow vertical aperture to the adjustable lens and diffraction grating. The vertical spectral lines are then projected onto the white surface of the photodetector apparatus. The target material in the photodetector can be revealed by rotating the black tube that connects the white surface to the apparatus. The target material is visible as a small black square inside of the apparatus, with the black tube opened. The mercury spectrum was then focused and aligned onto the photodetector. This was done by rotating the spectrometer until a spectral line fell directly on the cutout in the white surface of the photodetector. The lens and diffraction grating were then adjusted on the mercury vapor lamp, so that the spectral line was as bright as possible. The photodetector was then opened via rotating the black tube and rotated along its optical mount so that the light traveling through the cutout on the white surface fell squarely on the photodiode of the target material. Once verified, the black tube was closed and the alignment of the spectrometer was complete.

2. Procedure

To begin, we turned the mercury vapor lamp on to allow it to warm up. It is important that the mercury

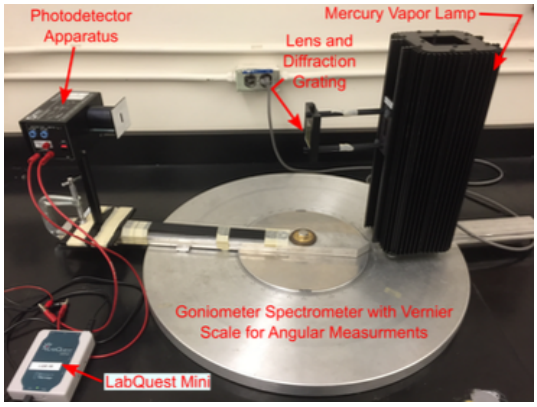

FIG. 1: Goniometer spectrometer apparatus

lamp remains on for the duration of the experiment, as the lifetime of the mercury discharge tube is dictated by the number of on/off cycles. In order to explore the photoelectric effect, there were two independent variables that were manually adjusted. The intensity of spectral lines incident on the detector, and the wavelength of the incident light. By rotating the goniometer spectrometer, we could select different wavelengths of the mercury spectrum. By using the variable transmission filter, we could change the intensity of the spectral lines. Changing these independent variables allowed us to measure the dependent variable V_0, the stopping potential. This reading was not immediate, as after zeroing the photodetector, the output potential asymptotes up to V_0 as the capacitor charges. In order to confirm the prior observations with this apparatus, we had to explore multiple wavelengths of the mercury light. We measured blue, green, yellow, and red spectral lines. We also took secondary wavelength measurements using the corresponding blue, green, yellow, and red filters to block out ambient light that could pollute the spectral lines. The stopping potential for each of these measurements was recorded, and their corresponding frequency value was calculated using Eq. 7. From this data, we can see the relationship between frequency and stopping potential. We can also see how the data differs when using the corresponding light filters. Using Python, the filtered and unfiltered stopping potential data was plotted against the calculated frequency. With the data in the form of Eq. 4, a linear least-squares fitting algorithm was used to extract the slope as h/e, which allows for the calculation of Plancks constant. For the intensity exploration, we selected the blue spectral emission line. Using the variable transmission filter, we took stopping potential measurements for 20%, 40%, 60%, 80%, and 100%, which represents what percent of light was blocked by the filter. From this data, we can explore how stopping potential changes with the intensity of the incident light.

B. Photoconductivity

This exploration involves a sample of photoconductive material, such as Cadmium Sulfide. Equipment for this experimental setup are described below.

- Cadmium Sulfide Photoconductive Material
- Optical Bench Set
- Light Source with holder
- Polarizer with holder
- Analyzer with holder
- LDR Module holder
- Power Supply 0-15V, 200mA
- Power Supply for light source
- Digital Multimeter

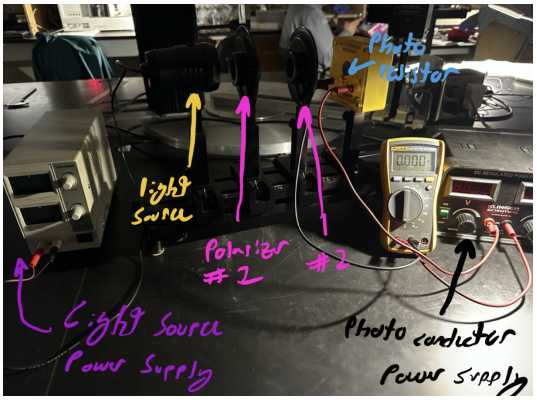

FIG. 2: Photoconductor Experimental Setup

To set up the experiment, we mounted the light source holder onto the optical bench. The light source was secured to its mount, ensuring its alignment with the optical axis. The polarizer and analyzer were placed between the light source and photoresistor (LDR module). The polarizer is used to initially polarize the light source, and the analyzer is essentially a second polarizer that modulates the intensity of the light according to Malus' law. Once the polarizer and analyzer were mounted, the photoresistor was placed onto the optical bench. It was connected to the power supply to control the applied voltage across the photoconductor. The light source, polarizer, analyzer, and LDR should all be aligned the same optical path. An image of the experimental setup can be found in Fig. 2.

There were three main goals to explore within this experiment. Voltage dependence, verifying photocurrent intensity dependence, and Wall-plug efficiency measurement of the photoconductor. As such the procedure will be split into three parts, outlining the methods used for each goal.

1. Measuring the Characteristic Curve of the Photoconductor

The main goal was to find how the applied voltage (bias) across the photoconductor affects the photocurrent under a constant intensity, creating a characteristic current-voltage curve for the photoresistor. The light source was powered on, and the polarizer and analyzer were both set to an angle of $\theta = 0°$. With the intensity fixed, the voltage was varied across the LDR, and the photocurrent generated in the LDR and the associated voltage were recorded using a multimeter every 0.001 amps. Thus we recorded how many volts returned a photocurrent of 0.001 to 0.010, recording voltage values every 0.001 amps. This process was then repeated at different analyzer angles, specifically $\theta = 30°, 60°, 90°$ to observe changes in the photocurrent under varying light intensities. The photocurrent vs. the applied voltage for each angle was then plotted in excel to illustrate the characteristic curves of the photoconductor under varying intensity levels.

2. Verification of Photocurrent Intensity Dependence via Malus' Law

The goal was to observe how the photocurrent varies as a function of intensity for a fixed applied voltage, emphasizing the cosine-squared relationship to Malus' Law. We set the voltage applied to the LDR as 7.06V, which was sufficient to produce a measurable photocurrent without exceeding the module's limits. The angle was varied between the polarizer and analyzer in increments of 10°, from 0° to 90°. At each angle, the photocurrent was recorded. According to Malus' law, the incident light intensity I on the photodetector should follow $I \propto cos^2(\theta)$, where θ is the angle between the polarizers axis and the direction of the polarized light. The recorded angles can then be used to calculate $cos^2(\theta)$ values representing the intensity I at each angle. The photocurrent i_p vs. $cos^2(\theta)$ was then plotted in excel to check for a linear relationship in order to verify Eq. 13.

3. Wall-Plug Efficiency Measurement of the Photoconductor

The main goal was to calculate the efficiency with which light is produced from electrical energy, and subsequently converted by the photodetector back into electrical current. To do so, the voltage V_{bulb} and the current I_{bulb} supplied to the light source were measured in order to calculate the power input P_{in}. A constant voltage bias V_{bias} was applied across the photoconductor. The photocurrent I_{photo} generated by the photoconductor under the fixed intensity was then recorded. The power output P_{out} from the photoconductor was then calculated. The wall-plug efficiency η of the light source and photoconductor system in converting electrical energy into light energy and back was then found. This process was repeated multiple times under consistent conditions to average the efficiency values.

IV. RESULTS

A. Photoelectric Effect

1. Confirming Previous Observations

As outlined in III A 2, the stopping potential for the filtered and unfiltered spectral lines was measured, and plotted against the calculated frequency. For ease of readability, the frequency values were translated to wavelength values in the plot, but all calculations were done using the associated frequency values. This plot can be observed in Fig. 3. According to the data, as the

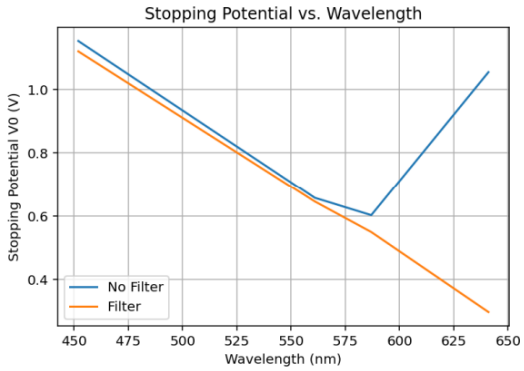

FIG. 3: Stopping Potential vs. Wavelength

wavelength increases, the stopping potential decreases. The difference between the filter and unfiltered data can also be observed, showing that for some wavelengths of light there was more ambient noise that threw off the stopping potential measurements. As such, the filtered data was used for all calculations to minimize the noise in each spectral emission line. The data shows that at long wavelengths (low frequency), the stopping potential eventually drops to zero, which means that no electrons are emitted. This confirms that there is some cutoff frequency where photoemission does not occur, regardless of the emission intensity. We also observed that when we decreased the light intensity using the variable transmission filter, the stopping potential took longer to reach its constant value. However this did not shift the frequency at which photoemission stops. The only thing that changed was the time to reach maximum stopping potential, while the cutoff wavelength stayed the same. This confirms that the incident light intensity does not change the threshold frequency of the plate material. Since the stopping potential took longer to reach when we lowered the intensity of light, this must mean that

fewer electrons were ejected. Fewer electrons would mean more time to reach the stopping potential, which is what we observed. This supports the idea that intensity effects the number of electrons, not their individual energy. As the data outlines in the plot, the stopping potential changes depending on the frequency. The stopping potential is related to the maximum kinetic energy through $K_{max} = eV_0$. So if the stopping potential is independent of light intensity, then the maximum kinetic energy is also independent of light intensity.

2. *Planck's Constant and Error Analysis*

After using the built in np.polyfit(...,cov=True) function to extract the slope of the plot in the form of h/e, Planck's constant was extracted by scaling by elementary charge e. To determine the uncertainty in the slope, the covariance matrix returned from the linear regression was used. This matrix contains information about how the slope and intercept vary due to fluctuations in the data. The diagonal elements of the covariance matrix represent the variances of the individual fit parameters. By taking the square root of the variance associated with the slope (the top-left element of the covariance matrix), we obtained the standard deviation, which is the uncertainty in the slope. This uncertainty was then scaled by e to obtain the uncertainty in Planck's constant. The uncertainty in h is then given by:

$$\delta h = e\sqrt{Var(m)} \tag{15}$$

Where m is the fitted slope, and e is the elementary charge of an electron. Thus our calculated value of Planck's constant was $(6.503 \pm 0.51) \times 10^{-34}$ joule seconds.

B. The Photoconductivity

1. *Voltage Dependence*

We varied the voltage bias across the CdS sample, and observed that as the amperage increased, the voltage increased as well. This confirms a linear relationship, and it also confirms that the system acts as an Ohmic circuit. A plot formed in excel of the V-I plot can be found in Fig. 4. We also varied the angle to see if it had any affect on the voltage, and found that as the angle increased, the slope of the V-I plot also increased. However at 90°, the slope falls flat as this means that no light was able to get through the polarizer, thus there was no voltage reading. Each angles corresponding slope can be seen in the plot. It is also worth noting that for the 60° curve, the line stops earlier than the others. This was because the maximum voltage for each current reading was much larger than the other angle curves, and we stopped taking measurements around 10V, as we did not want to overload the LDR module. We also took enough data trials to ensure that the trends could be seen in each angle, making up for the lack of maximum voltage measurements in the 60° curve.

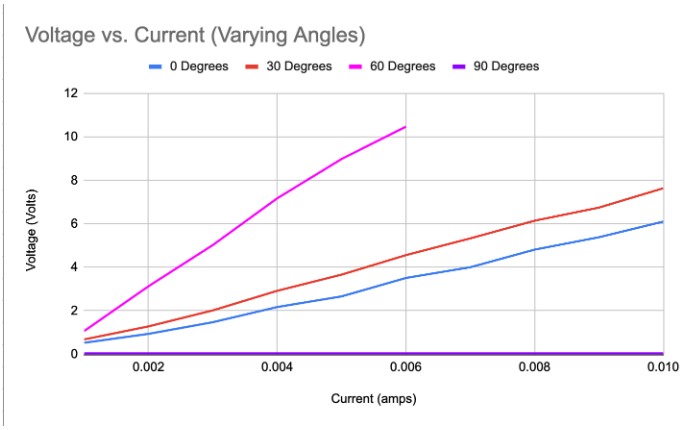

FIG. 4: Voltage vs. Current with varying Angles

2. *Intensity Dependence*

According to Malus' Law, $I \propto cos^2(\theta)$. As such, the illumination intensity was varied while the voltage was kept constant. The photocurrent was plotted against $cos^2(\theta)$ with θ being the associated change in angle. The plot can be seen in Fig. 5. According to the plot,, the photocurrent has a linear relationship with the intensity, verifying its dependence according to Malus' law.

3. *Wall-Plug Efficiency Assessment*

We calculated the efficiency with which the electrical power into the light source is converted into photons, then subsequently converted by the photoconductor back into electrical current. With the voltage being held constant, we found the efficiency to be 0.0088. When we increased the voltage bias, the efficiency changed to 0.078. This increase is likely due to stronger electric fields enhancing charge carrier collection, thus increasing the photocurrent. However when we decreased the input voltage, the efficiency increased even further to 0.191. This suggest that while the absolute current may be lower at lower voltages, the reduced power input leads to a more favorable ratio of output current to input power. These results indicate that the higher operating voltages do not necessarily yield a better efficiency, and the optimal performance in photoconductive systems requires balancing both power output and input.

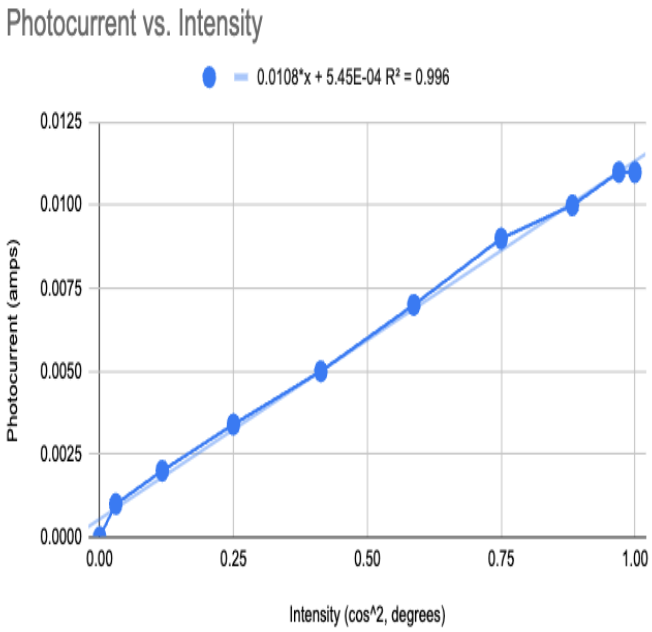

FIG. 5: Voltage vs. Current with varying Angles

V. DISCUSSION AND CONCLUSIONS

This experiment aimed to explore the photoelectric effect, and the photoconductivity of a Cadmium Sulfide sample. Beginning with the photoelectric effect our experiment aimed to confirm key properties Einstein postulated, such as the relationship between light wavelength, frequency, and the stopping potential, as well as measuring Plancks constant. As expected, the stopping potential decreases with increasing wavelength (or decreasing frequency), which is consistent with the theoretical predictions of the photoelectric effect. Our plot also uncovers a noticeable trend where the stopping potential drops to zero at long wavelengths, indicating some cutoff frequency below which photoemission stops occurring. Furthermore, when the light intensity was reduced using a variable transmission filter, the time taken for the stopping potential to reach a constant value increased. This suggests that fewer electrons were being emitted due to the lower intensity, although the cutoff frequency remained unchanged. This finding supports the conclusion that light intensity affects the number of emitted electrons, but not their individual energy. Since the stopping potential V_0 is independent of incident light intensity, the maximum kinetic energy of the emitted electrons given by $K_{max} = eV_0$, is also independent of light intensity. Thus this objective was successful in verifying the core principles of the photoelectric effect. Additionally, this objective also highlighted the impact of ambient noise, which affected the accuracy of stopping potential measurements at certain wavelengths (especially red) as seen in Fig. 3. To mitigate this affect, wavelength specific filters were utilized, showing a much more reasonable trend in the plot. This turned out to be a successful fix, as the filtered data was utilized in the other goal for the photoelectric effect exploration, calculating Plancks constant. Our calculated value came out to be $(6.503 \pm 0.51) \times 10^{-34}$ joule-seconds, which is extremely close to the nominal value of 6.626×10^{-34} joule-seconds, exhibiting a percent error of only 1.86%. This means that our experimental procedure was sufficient to measure Plancks constant with high accuracy, as well as verifying key properties of the photoelectric effect.

The next main objective of this experiment was exploring the photoconductivity of a Cadmium Sulfide (CdS) sample. The main goals were to explore voltage dependence, intensity dependence, and a wall-plug efficiency assessment. First the voltage bias was varied across the CdS sample, and the resulting current was measured. The data showed a linear relationship between the voltage and current, confirming an Ohmic behavior. This was visualized in the V-I plot in Fig. 4. We also varied the angle of the incident light, and observed that as the angle increased, the slope of the V-I curve increased as well. At 90° the slope flattened, confirming that no light was transmitted through the polarizer and thus no photoconductivity occurred. However $0°, 30°,$ and $60°$, the slope increased respectively, consistent with the expected behavior of polarized light passing through a polarizer. Secondly, we investigated the intensity dependence of the CdS sample. Malus' Law states that the transmitted light intensity should vary as $cos^2(\theta)$. By plotting the photocurrent versus $cos^2(\theta)$, we observed a clear linear relationship as seen in Fig. 5, confirming that the photocurrent is directly proportional to the light intensity. This further validates the CdS sample's expected response to varying illumination, as well as verifying Malus' Law. The last goal was to asses the wall-plug efficiency of the system which we found at a constant voltage to be 0.0088. Increasing the voltage bias led to an efficiency of 0.078, likely do to stronger electric fields improving carrier collection. However interestingly, lowering the input voltage led to an even higher efficiency of 0.191, which suggested that although the absolute current was lower in the system, the reduced power input made the overall power ratio more favorable. These results indicate that maximizing photocurrent alone is not sufficient for optimal operation in the given setup. Instead, balancing the power input and output is necessary to achieve high wall-plug efficiency.

Overall this experiment not only confirmed Einstein's predictions about the photoelectric effect, specifically that the energy of emitted electrons depends solely on the frequency of incident light and not its intensity, but it also provided a detailed verification of several important concepts in quantum mechanics and semiconductor physics. From the stopping potential measurements, we validated the existence of some threshold frequency. Electrons were only ejected when the incoming photons had sufficient

energy, supporting the idea from quantum mechanics that light consists of small discrete energy packets called "photons," rather than the contentious wave from classical physics. Furthermore, our observations support the claim that light intensity affects the number of electrons emitted, but not their individual energies. This directly reinforced Einstein's idea that photon energy is independent of light intensity, refuting the classical expectation that higher light intensity would transfer more energy to electrons. The confirmation that the maximum kinetic energy of emitted electrons is also independent of intensity, and instead is related to photon frequency provides further evidence that the photoelectric effect is a quantum phenomena. In the photoconductivity exploration in the experiment, the voltage dependence showed that the illuminated CdS sample behaved Ohmically within the test range. This is a fairly essential finding for designing semiconductor based light sensors, where a predictable electrical behavior is needed. The intensity dependence investigation confirmed that the photocurrent varied linearly with the cosine squared of the angle of polarization, verifying Malus' Law, a classical optics principle. Together, these experiments provided a detailed view of the interactions between light and matter, combing quantum theory with material science applications. Our results not only confirmed Einsteins predictions of light, but also helped bridge the gap between quantum physics and material science, specifically showing how quantum effects scale up to influence electrical properties in materials, such as the Cadmium sulfide sample. The results from this experiment connect with so many real-world technologies. Applications of these principles span across many fields in our modern world, from solar panels, optical communication systems, medical imaging, and even quantum computing. These results also reflect on one of the most significant breakthroughs in science: the birth of quantum physics. This fundamentally continues to change our understanding of the universe, and is still paving the way for new revolutionary technologies, simply from Einstein exploring the photoelectric effect.

VI. ACKNOWLEDGMENTS

Both group members did the experiment and data analysis. James Atkisson wrote the Methods, Results, Abstract, Discussion and Conclusion sections. Zhongzhe Li wrote the introduction and theory sections. ChatGPT was consulted for specific LaTeX syntax for images as well as equations. Dextify was used to find out specific symbols as well.